HTML ABSTRACT + LINKS

JOURNAL OF APPLIED PHYSICS VOLUME 96, NUMBER 6 15 SEPTEMBER 2004

Structure and optical properties of cored wurtzite (Zn,Mg)O heteroepitaxial nanowires

Y. W. Heo, C. Abernathy, K. Pruessner, W. Sigmund, and D. P. Norton[a)]
Department of Materials Science and Engineering, University of Florida, P.O.Box 116400, Rhines Hall, Gainesville, Florida 32606

M. Overberg
Sandia National Laboratory, P.O. Box 5800, Albuquerque, New Mexico 87185-0603

F. Ren
Department of Chemical Engineering, University of Florida, Gainesville, Florida 32606

M. F. Chisholm
Oak Ridge National Laboratory, P.O. Box 2008, Oak Ridge, Tennessee 37831

(Received 3 November 2003; accepted 31 May 2004)

The synthesis, structure, and optical properties of one-dimensional heteroepitaxial cored (Zn,Mg)O semiconductor nanowires grown by a catalyst-driven molecular beam epitaxy technique are discussed. The structures form spontaneously in a Zn, Mg and O_2/O_3 flux, consisting of a single crystal, Zn-rich $Zn_{1-x}Mg_xO(x<0.02)$ core encased by an epitaxial $Zn_{1-y}Mg_yO(y\gg 0.02)$ sheath. High resolution Z-contrast scanning transmission electron microscopy shows core diameters as small as 4 nm. The cored structure forms spontaneously under constant flux due to a bimodal growth mechanism in which the core forms via bulk like vapor-liquid-solid growth, while the outer sheath grows as a heteroepitaxial layer. Temperature-dependent photoluminescence shows a slight blueshift in the near band edge peak, which is attributed to a few percent Mg doping in the nanoscale ZnO core. The catalyst-driven molecular beam epitaxy technique provides for site-specific nanorod growth on arbitrary substrates. © *2004 American Institute of Physics*. [DOI: 10.1063/1.1774257]

I. INTRODUCTION

The synthesis and properties of one-dimensional (1D) semiconductor nanowire structures is of significant interest.[1] In recent years, nanowire growth has been reported using several techniques,[2,3] and has included numerous semiconductors,[4,5] including the oxides Ga_2O_3,[6] In_2O_3,[7] SnO_2,[8] and ZnO.[9] Despite significant progress, major challenges in the manipulation of nanowire materials remain. The fabrication of integrated systems using nanowire material requires the site-specific growth or placement of nanowires on relevant device platforms. In addition, the formation of complex, multicomponent structures and interfaces are needed for low-dimensional structures and electronic devices. In thin-film semiconductor research, the formation of heteroepitaxial interfaces has proven to be useful in the development of numerous device concepts, as well as in the investigation of low-dimensional phenomena.[10] Unfortunately, such heterostructures have rarely been realized outside of the conventional 2-D planar thin-film geometry.[11] Nevertheless, the synthesis of 1D linear heterostructures is scientifically interesting and potentially useful, particularly if a technique is employed that allows for spatial selectivity in nanowire placement. Addressing these challenges could prove useful in realizing integrated device functionality involving semiconducting nanowires for a number of applications, including nanoscale electric field-effect transistors,[12] single electron transistors,[13] biological and chemical sensors,[14] electron emitters,[15] optical emitters and detectors.[16,17]

In this paper, the properties of 1-D heteroepitaxial structures are described. In particular, the structural and optical properties of cored (Zn,Mg)O nanowires, formed via self-assembled bimodal growth, are discussed. ZnO is among the more interesting and important semiconducting oxides.[18] ZnOis an n-type, direct band gap semiconductor with $E_g = 3.35$ eV. Electron doping via defects originates from Zn interstitials in the ZnO lattice. The intrinsic defect levels that lead to n-type doping lie ≈ 0.05 eV below the conduction band. The room temperature Hall mobility in ZnO single crystals is among the highest for the oxide semiconductors, on the order of 200 $cm^2V^{-1}\,s^{-1}$. The exciton binding energy for ZnO is on the order of 60 meV, yielding efficient luminescence at room temperature. The synthesis of ZnO nanowires and nanorods has been demonstrated using vapor-phase transport via a vapor-liquid-solid mechanism,[19] gas reactions,[20] and oxidation of metal in the pores of anodic alumina membranes.[21] Room-temperature ultraviolet lasing via optical pumping has been demonstrated with ZnO nanorods on deposited Au catalyst using a high-temperature vapor transport process.[16] Recently, we reported on catalyst-driven molecular beam epitaxy (MBE) of ZnO nanorods.[22] The process is site specific, as single crystal ZnO nanorod growth is realized via nucleation on Ag films or islands that are deposited on a SiO_2-terminated Si substrate surface. Growth occurs at relatively low substrate temperatures, on

[a)]Author to whom correspondence should be addressed; electronic mail: dnort@mse.ufl.edu

 © 2004 American Institute of Physics

Downloaded 28 Sep 2004 to 134.76.92.150. Redistribution subject to AIP license or copyright, see http://jap.aip.org/jap/copyright.jsp

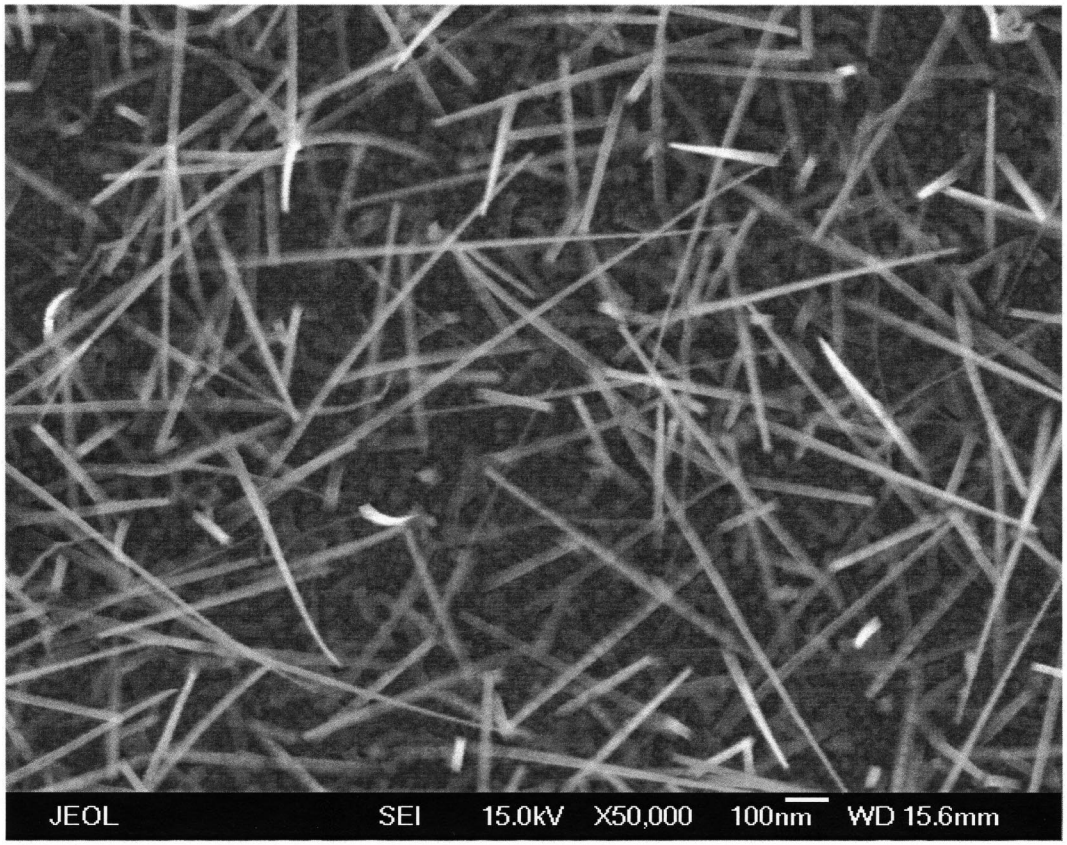

FIG. 1. Field-emission scanning electron microscopy image of cored (Zn,Mg)O nanorods grown on Ag-coated Si. The conditions for growth were $T_g = 400°C$ Zn pressure $=3\times10^{-6}$ mbar, Mg pressure $=4\times10^{-7}$ mbar, O_2/O_3 pressure $=5\times10^{-4}$ mbar. The Mg source was shuttered with a 60 s open/ 60 s closed cycle.

the order of 300–500 °C, making it amenable to integration on numerous device platforms. With this approach, nanorod placement can be predefined via location of metal catalyst islands or particles.

II. EXPERIMENTAL DETAILS

The heteroepitaxial cored nanostructures described here are based on the (Zn,Mg)O alloy system, and were synthesized using the catalysis-driven molecular beam epitaxy method. Details of the growth experiments are reported elsewhere. An ozone/oxygen mixture was used as the oxidizing source. The cation flux was provided by Knudsen effusion cells using high purity (99.9999%) Zn metal and Mg (99.95%) as the source materials. The substrates were Si wafers with native SiO_2 terminating the surface. No effort was made to remove the native oxide or to terminate the surface with hydrogen.

III. RESULTS AND DISCUSSION

Site-selective nucleation and growth of cored nanorods was achieved by coating Si substrates with Ag islands. For a nominal Ag film thickness of 20 Å, discontinuous Ag islands are realized. On these small metal catalyst islands, (Zn,Mg)O nanorods were observed to grow. Figure 1 shows an FE-SEM micrograph of these nanorods, indicating a length approaching 1 μm. The growth temperature was 400 °C. Energy-dispersive spectrometry confirmed the presence of Mg in the nanorod composition, as seen in Fig. 2. Typical growth times for (Zn,Mg)O on the Ag-coated silicon was 2 h with growth temperatures ranging from $T_g = 300-500°C$. The site specificity for nanowire growth using this technique is evident in Fig. 3, showing FE-SEM images of (Zn,Mg)O nanorods on a Ag-patterned substrate grown in a Znpressure of 3×10^{-6}mbar, a Mg pressure of 4×10^{-7} mbar, and an O_2/O_3 pressure of 5×10^{-6} mbar. (Zn,Mg)O nanorods form only on the Ag-coated regions. The potential for growing single nanorods on selected locations is exemplified in Fig. 4, where single ZnO nanorods are nucleated on Ag nanoparticles dispersed on a SiO_2-terminated Si surface. In order to acquire these images,

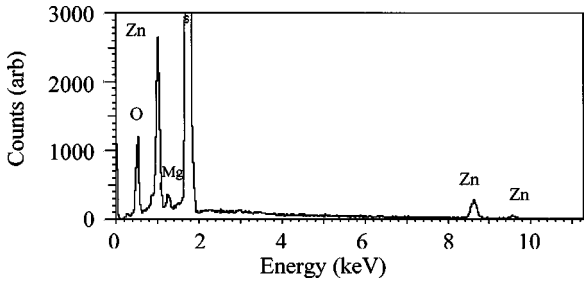

FIG. 2. Energy dispersive spectrometry data for (Zn,Mg)O nanorods.

Downloaded 28 Sep 2004 to 134.76.92.150. Redistribution subject to AIP license or copyright, see http://jap.aip.org/jap/copyright.jsp

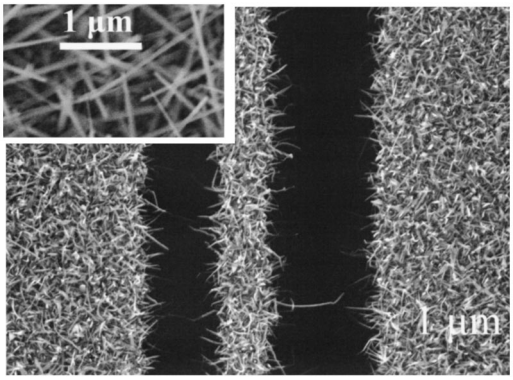

FIG. 3. Field-emission scanning electron microscopy image of cored (Zn,Mg)O nanorods grown on a patterned Ag-coated Si substrate. The conditions for growth were T_g=400°C Zn pressure =3×10^{-6} mbar, Mg pressure =4×10^{-7} mbar, O_2/O_3 pressure =5×10^{-4} mbar. Note that (Zn,Mg)O nanorod nucleation occurs only on the catalyst-coated regions.

the sample was coated with a thin layer of carbon to avoid charging effects. From the high-resolution image, the nanorod cross section appears to be cylindrical, although any faceting of the side walls may be obscured by the carbon coating. The thickness of the nanorods shown is on the order of 30 nm, although the carbon coating may exaggerate this thickness.

The formation of the (Zn,Mg)O nanorods includes the v-1-s mechanism described earlier, although heteroepitaxial growth occurs as well as will be seen. Figure 5 shows a Z-contrast scanning transmission electron microscopy (Z-STEM) image of an individual (Zn,Mg)O nanorod grown at 400°C, with a Zn pressure of 3×10^{-6} mbar, a Mg pressure of 4×10^{-7} mbar, and an O_2/O_3 pressure of 5×10^{-4} mbar. The Mg flux was cycled on and off every 60 s, which was inconsequential to the nanorod structure. Evident in the image is a small particle embedded at the tip of the rod. This is similar to what is observed for other nanorod synthesis that is driven by a catalytic reaction, where catalyst particles become suspended on the nanorod tip. The diameter of the catalyst particle is ~6 nm. Note that, at the nanorod tip, the contrast in the Z-STEM image is relatively uniform, indicating uniform cation distribution. However, the rod diameter is

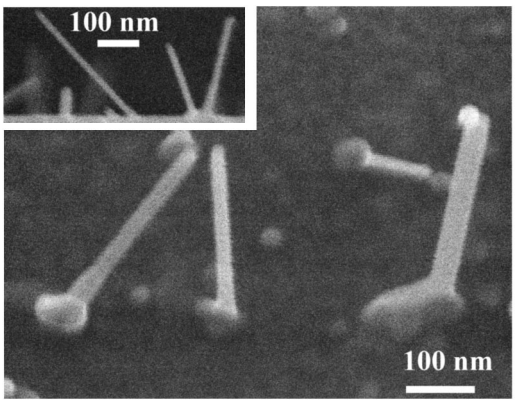

FIG. 4. Field-emission scanning electron microscopy image of individual ZnO nanorods grown on Ag nanoparticles dispersed on the Si substrate.

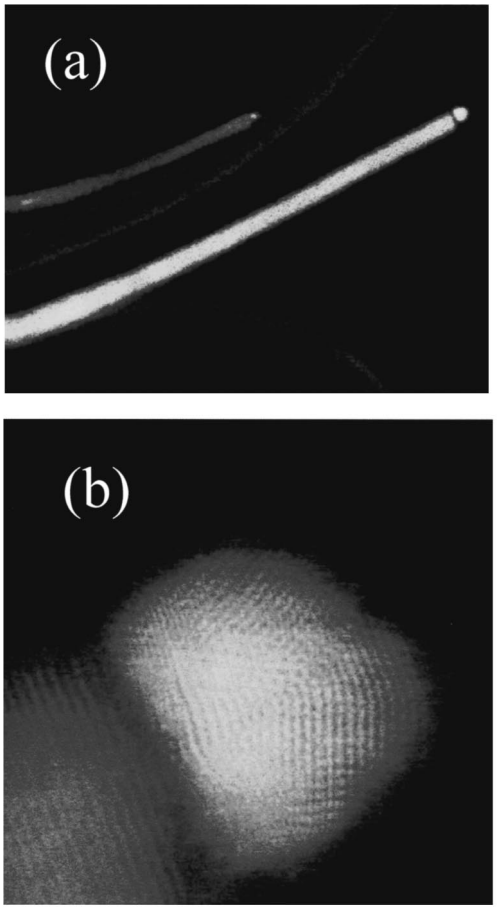

FIG. 5. Z-contrast scanning transmission electron microscopy image (a) of a (Zn,Mg)O nanorod with (b) a Ag catalyst particle at the rod tip.

also tapered along the length, being thicker at the base than on the tip, with an average diameter on the order of 10 nm.

As reported elsewhere, a radial segregation of the Zn and Mg occurs during growth.[23] A Zn-rich core surrounded by a Mg-rich sheath is observed as seen in Fig. 6. As discussed elsewhere, in bulk material, the solubility of Mg in ZnO is relatively low, on the order of 4 at %.[24] In contrast, Mg content as high as $Zn_{0.67}Mg_{0.33}O$ has been reported to be metastable in the wurtzite structure for epitaxial thin films. For this composition, the band gap of ZnO can be increased to ~3.8 eV. For (Zn,Mg)O nanorod growth, it appears that both (hence bimodal) growth modes are relevant, but for different regions in the rod. Under low temperature MBE growth conditions, a solubility-driven segregation occurs during the catalyst-driven core formation, with the core composition determined by bulk solid solubility. Subsequently, an epitaxial sheath grows with Mg content and crystal structure determined by epitaxial stabilization. The net result is the growth of (Zn,Mg)O nanorods that are not uniform in composition across the diameter, but distinctly cored. Figure 6 shows a high resolution Z-STEM image of a nanorod grown under the conditions described. The lattice image for the nanorod specimen indicates that the rod is crystalline with the wurtzite crystal structure maintained throughout the cross section. The *c* axis is oriented along the long axis of the rod. The higher contrast for the center core region clearly

Downloaded 28 Sep 2004 to 134.76.92.150. Redistribution subject to AIP license or copyright, see http://jap.aip.org/jap/copyright.jsp

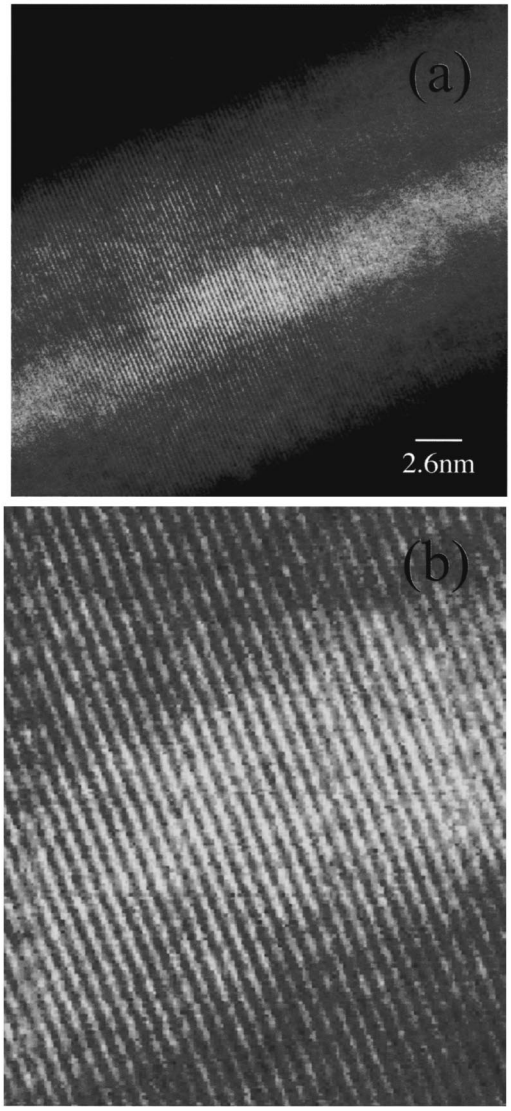

FIG. 6. Z-contrast scanning transmission electron microscopy images of cored (Zn,Mg)O nanorods. The high contrast of the core (a) indicates a significantly higher Zn content for the core relative to the sheath. The higher resolution image (b) of the core indicates the wurtzite structure for the core and sheath material.

indicates a higher cation atomic mass. The structures consist of a zinc-rich $Zn_{1-x}Mg_xO$ core (small x) surrounded by a $Zn_{1-y}Mg_yO$ (large y) sheath containing higher Mg content.

While the nanorod imaged in Fig. 6 is crystalline across the entire cross section, other rods exhibit sheath properties that vary along the length. In particular, consider the nanorod shown in Fig. 7. In this case, the core and sheath are both crystalline in one region of the rod. However, as one proceeds along the length, the crystallinity changes. In particular, for the rod considered, the sheath region becomes either polycrystalline or amorphous as one approaches the rod tip. Still further down the nanowire, the image suggests a lack of crystallinity for both the core and sheath, although the lack of crystallinity in the sheath may effectively obscure imaging of the core region. This change in crystallinity change along the length of the rod may reflect the fact the temperature gradient will develop along the nanowire length during

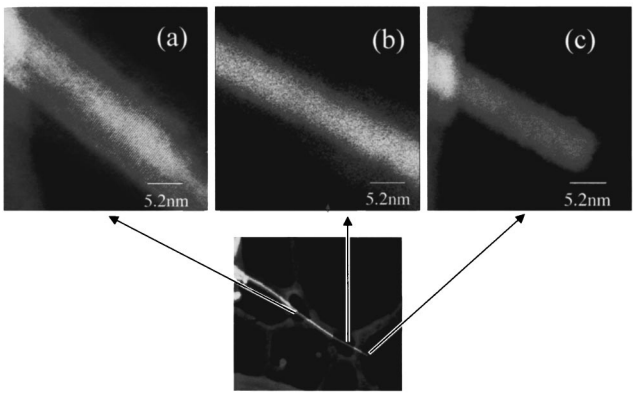

FIG. 7. Z-contrast scanning transmission electron microscopy image of regions of a nanorod showing (a) a crystalline core and sheath, (b) an amorphous sheath, and (c) an amorphous sheath with no evidence of crystallinity in the core.

growth. This occurs since the substrate is the source of heat during nanorod formation. Sheath material deposited on the tip of longer rods during the latter part of the synthesis process will do so at a lower local temperature than the material closer to the substrate.

In order to assess crystalline quality and investigate possible quantization effects, the optical properties of the cored nanorods were examined using photoluminescene. Spectra were taken over the temperature range 6 K–300 K. A He-Cd (325 nm) laser was used as the excitation source. For the low temperature measurements, the sample was cooled using either a helium flow or closed cycle cryostat. Figure 8 shows the photoluminescence spectra taken at various temperatures for the cored nanorod specimens. For ZnO rods (no Mg), the photoluminescene results are consistent with luminescence reported for near band edge emission in crystals,[25]

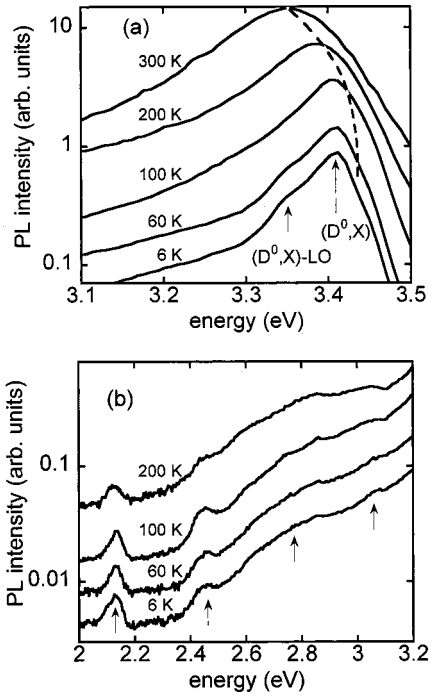

FIG. 8. Photoluminescence at various temperatures for (a) near band edge and (b) visible emission from cored (Zn,Mg)O nanorods.

Downloaded 28 Sep 2004 to 134.76.92.150. Redistribution subject to AIP license or copyright, see http://jap.aip.org/jap/copyright.jsp

epitaxial films,[26] and larger diameter ZnO nanorods.[27] The free exciton emission dominates luminescence, with a room temperature peak at 3.30 eV. At room temperature, the spectra for the cored (Zn,Mg)O nanorods is also dominated by the free exciton luminescence. However, the peak in luminescence at room temperature is at 3.35 eV, which is blueshifted relative to that seen in pure ZnO (peak at 3.30 eV). As the temperature is decreased, the free exciton emission shifts to higher energy due to the temperature dependence of the band gap. At the lower temperatures, the donor-bound exciton (D^0,X) dominates luminescence.[26] Also seen at low temperatures is a peak at 3.35 eV, which is assigned as the corresponding longitudinal optical phonon replica (D^0,X)-LO. At lower energies, at least four relatively weak peaks are also observed in the visible spectrum, indicated by arrows in the figure. Similar peaks have been reported elsewhere for bulk and thin-film ZnO materials.[25,26]

Blueshifts in the near band edge luminescence for nanoscale semiconducting structures can reflect quantum confinement effects. With a band gap range of 3.2–3.8 eV, the ZnO/(Zn,Mg)O heterostructure system affords the opportunity to realize electron confinement due to band offsets. In semiconductors, the onset of reduced dimensionality effects should be observable for structures with dimensions below the relevant length scales. Quantization of the electron states should be observable for low dimensional structures with length scales on the order of the exciton Bohr diameter.[28,29] A significant blueshift in the near-band edge emission was previously observed for InP nanorods with diameters approaching that of the exciton diameter.[30] For ZnO, the exciton Bohr diameter is 34 Å, which is approximately equal to the core diameters considered. Shifts in the near-band edge photoluminescence peak energy have been observed for 0-D ZnO nanoparticles diameters on the order of 2–6 nm.[31] For ZnO/(Zn,Mg)O superlattices, quantum confinement effects are predicted for well widths less than ~5 nm, and are reported for ZnO layer thicknesses less than ~4 nm.[29] ZnO/(Zn,Mg)O superlattices with a ZnO well width of 3.1 nm show a 100 meV blueshift in near-band edge luminescent peak energy.[29] In the present work, a 50 meV shift is observed for the 1-D nanorod cored structure, the core diameter (4 nm) being roughly equivalent to the bulk exciton diameter (3.4 nm). While a blueshift in near-edge emission is consistent with expected quantum confinement in 4 nm diameter ZnO cores, one cannot easily differentiate this from a similar blueshift that would result from a few percent doping of Mg in the core regions. However, from the Mg dependence of the band edge peak,[23] it appears that quantization effects on the PL shift are minimal.

Fundamentally, these 1-D ZnO nanostructures provide an attractive system for probing low-dimensional effects such as quantization, interface scattering, and ballistic transport. The relatively low growth temperatures suggest that cored (Zn,Mg)O nanorods could be integrated on device platforms for numerous applications, including chemical sensors, nano-optics, scanning probes, and nanoelectronics. More generally, the spontaneous bimodal growth mode demonstrated for (Zn,Mg)O may prove applicable in the synthesis of heteroepitaxial cored nanowire-materials where thermodynamics and epitaxy impose different cation or anion solubility limits.

ACKNOWLEDGMENTS

The work done at the University of Florida was supported by the Army Research Office through Grant No. DAAD19-01-1-0603 and the National Science Foundation through Grant No. DMR-0305228. The work done at ORNL was sponsored by U.S. Department of Energy under Contract No. DE-AC05-00OR22725. The authors would also like to thank the Major Analytical Instrumentation Center, Department of Materials Science and Engineering, University of Florida.

[1] H. Sakaki, J. Cryst. Growth **251**, 9 (2003).
[2] Y. Wu and P. Yang, Chem. Mater. **12**, 605 (2000).
[3] A. M. Morales and C. M. Lieber, Science **279**, 208 (1998).
[4] R. Solanki, J. Hua, J. L. Freeouf, and B. Miner, Appl. Phys. Lett. **81**, 3864 (2002).
[5] R. Ragan, C. C. Ahn, and H. A. Atwater, Appl. Phys. Lett. **82**, 3439 (2003).
[6] H. Z. Zhang *et al.*, Solid State Commun. **109**, 677 (1999).
[7] D. Zhang, C. Li, S. Han, X. Liu, T. Tang, W. Jin, and C. Zhou, Appl. Phys. Lett. **82**, 112 (2003).
[8] J. K. Jian, X. L. Chen, W. J. Wang, L. Dai, and Y. P. Xu, Appl. Phys. A: Mater. Sci. Process. **76**, 291 (2003).
[9] Z. W. Pan, Z. R. Dai, and Z. L. Wang, Science **291**, 1947 (2001).
[10] F. Capasso, Science **235**, 172 (1987).
[11] L. J. Lauhon, M. S. Gudiksen, D. Wang, and C. M. Lieber, Nature (London) **420**, 57 (2002).
[12] J. U. Kim, and I. V. Krive, and J. M. Kinaret, Phys. Rev. Lett. **90**, 176401 (2003).
[13] N. J. Stone and H. Ahmed, Appl. Phys. Lett. **73**, 2134 (1998).
[14] Y. Cui, Q. Wei, H. Park, and C. M. Lieber, Science **293**, 1289 (2001).
[15] C. J. Lee, T. J. Lee, S. C. Lyu, Y. Zhang, H. Ruh, and H. J. Lee, Appl. Phys. Lett. **81**, 3648 (2002).
[16] M. H. Huang *et al.*, Science **292**, 1897 (2001).
[17] J. Wang, M. S. Gudiksen, X. Duan, Y. Cui, and C. M. Lieber, Science **293**, 1455 (2001).
[18] D. C. Look, Mater. Sci. Eng., B **80**, 383 (2001).
[19] M. H. Huang, Y. Wu, H. Feick, N. Tran, E. Weber, and P. Yang, Adv. Mater. (Weinheim, Ger.) **13**, 113 (2001).
[20] C. C. Tang, S. S. Fan, M. L. de la Chapelle, and P. Li, Chem. Phys. Lett. **333**, 12 (2001).
[21] J. C. Hulteen and C. R. Martin, J. Mater. Chem. **7**, 1075 (1997).
[22] Y. W. Heo, V. Varadarajan, M. Kaufman, K. Kim, F. Ren, P. H. Fleming, and D. P. Norton, Appl. Phys. Lett. **81** 3046 (2002).
[23] Y. W. Heo, K. Pruessner, W. Sigmund, C. Abernathy, D. P. Norton, M. Overberg, F. Ren, M. F. Chisholm, Appl. Phys. A: Mater. Sci. Process. (submitted).
[24] J. F. Sarver, F. L. Katnack, and F. A. Hummel, J. Electrochem. Soc. **106**, 960 (1959).
[25] D. C. Reynolds, C. W. Litton, and T. C. Collins, Phys. Rev. **140**, A1726 (1965).
[26] M. Haupt, *et al.*, J. Appl. Phys. **93** 6252 (2003).
[27] W. I. Park, Y. H. Jun, S. W. Jung, and G.-C. Yi, Appl. Phys. Lett. **82**, 964 (2003).
[28] V. S. Dneprovskii, E. A. Zhukov, N. Yu. Markova, E. A. Mulyarov, K. A. Chernoutsan, and O. A. Shalygina, Phys. Solid State **42**, 544 (2000).
[29] A. Ohtomo, M. Kawasaki, I. Ohkubo, H. Koinuma, T. Yasuda, and Y. Segawa, Appl. Phys. Lett. **75**, 980 (1999).
[30] M. S. Gudiksen, J. Wang, and C. M. Lieber, J. Phys. Chem. B **106**, 2036 (2002).
[31] E. M. Wong and P. C. Searson, Appl. Phys. Lett. **74**, 2939 (1999).

Downloaded 28 Sep 2004 to 134.76.92.150. Redistribution subject to AIP license or copyright, see http://jap.aip.org/jap/copyright.jsp